

Flexural Behaviour of Concrete Beams Reinforced with Major Steel Bars under Normal and Corrosive Operational Conditions

Adekunle P. Adewuyi  and Gaolatlhe B. Eric 

Department of Civil Engineering, University of Botswana, Gaborone, Botswana

Corresponding author's Email: adewuyiA@ub.ac.bw

ABSTRACT

Quality assurance of construction materials is very fundamental for structural safety, reliability, serviceability, and durability of constructed civil infrastructure. Inflow of defective or substandard building and construction materials into the industry, particularly reinforcing steel bars, is responsible for many structurally deficient constructed facilities which often lead to failure or ultimate collapse of reinforced concrete (RC) structures. Characterization of steel rebars from two major manufacturers into Botswana construction industry, designated herein as M1 and M2, were conducted as a basis for the evaluation of the quality assurance and control of the products. The flexural behaviour of their respective RC beams, designated herein as B-M1 and B-M2, of dimension $150 \times 200 \times 3000$ mm and subject to four-point loading tests were determined under normal and artificially induced corrosion conditions to assess the influence of steel rebars M1 and M2 on the stiffness and load-carrying capacity. The average yield strengths of steel reinforcing bars were 427 N/mm^2 for M1 and 459 N/mm^2 for M2. The moduli of elasticity for M1 and M2 were 203 GPa and 205 GPa, respectively. The percentage elongation was found to be 7.93% for M1 and 7.24% for M2. The flexural strength of beams reinforced with M1 was 7% and 16.5% lower than RC beam with M2 under normal and accelerated corrosion of 5% of NaCl solution for 60 hours condition, respectively. The flexural behaviour of RC beams reinforced with B-M1 had a lower flexural strength under both normal and corrosive environmental conditions as compared to B-M2. The flexural strength of B-M1 had reduced from 48.5 N/mm^2 to 41.0 N/mm^2 , while B-M2 reduced from 52.2 N/mm^2 to 49.2 N/mm^2 . This represented loss of load-carrying capacity of 15.4% and 5.8% for B-M1 and B-M2 respectively due to exposure to corrosive environment. The findings revealed disparity in bending capacity due to the low interfacial bonding due to reduced relative rib areas. A more intensive quality control of imported steel should be ensured at the ports of entry by relevant regulatory agencies.

Keywords: Flexural capacity, Stiffness, Reinforcing bars, Relative rib area, Interfacial bonding, Accelerated corrosion, Ultimate load.

INTRODUCTION

Concrete, generally regarded as the oldest and most widely used construction material, plays a vital role in global infrastructural development and economic growth (Adewuyi et al., 2015). The preference for reinforced concrete (RC) as a construction material is influenced by its durability and fire resistance, structural versatility and formality, and the complementary properties between the reinforcing steel bars and concrete (Makul, 2020). Extensive studies have been carried out to investigate flexural behaviour of RC beams using three- or four-point loading with identical geometric dimensions and steel bar specimens (Qui et al. 2022; Adewuyi et al. 2015; Djmaluddin 2013; Li et al. 2020; Kim & Kim 2019; Ignjatovic et al. 2013). However, research gaps on this subject are yet to be filled to compare the performance of different reinforcing steel bars from different

manufacturers in tension and flexure, and under the influence of progressive corrosion, hence the need to do this study. Studies on flexural behaviour of RC elements are primarily focused on the failure modes, first cracking load, ultimate load, deflection, stiffness, ductility and crack patterns.

The process of corrosion of the reinforcements is recognized as the most predominant degradation mechanism of RC structures that leads to structural deterioration and functional failure (Verstryngge et al., 2022). Corrosion of reinforcing bars progressively and ultimately reduces capacity and the residual service life of the structure, thereby creating huge economical loss and environmental problems (Kunawisarut et al., 2024). Its enhancement of the RC section ductility is often as the expense of their long-term performance in the form of the loss of flexural strength, deformation behaviour, bond strength and different cracking modes (Peng et al., 2021).

RESEARCH ARTICLE
 PII: S225204302400033-14
 Received: June 25, 2024
 Revised: September 02, 2024
 Accepted: September 05, 2024

The products of corrosion process are a complex mixture of iron oxides, hydroxides and hydrated oxides that progress based on the local environmental condition (Adewuyi et al. 2022; Rodrigues et al., 2021). Early detection of corrosion and prompt maintenance could help reduce the life cycle cost thereby extending the service life of structures. Embedded steel rebars in concrete are often secured against corrosion during the service life of the structure by providing adequate nominal cover since concrete is both durable and resistant against corrosion and fire (Fouad et al., 2016). The progressive corrosion of RC flexural structures is illustrated by a uniform dissolution of the whole surface as shown in Figure 1a or by a local attack which is called ‘pitting’ corrosion when it is much localized as shown in Figure 1b. It may also manifest at the microscopic level as ‘inter- or trans-granular’ (Figure 1c) attack when metal grains are very locally affected.

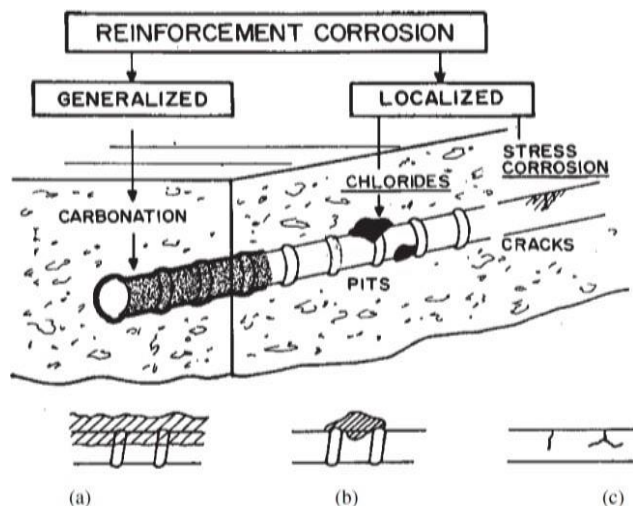


Figure 1. Categorization of corrosion of steel rebars as (a) carbonation, (b) chloride attack and (c) stress corrosion cracking.

Recent studies on corrosion of reinforcement in concrete structures were reported extensively in literature (Almusallam 2001; Bertolini et al. 2013; Hunkeler 2005; Patil et al. 2017). The effect of corrosion of reinforcement to tension stiffening results in local reduction of cross-sectional area of tension reinforcement leading to reduction of its stiffness, bond strength and therefore the change contribution of concrete in tension between cracks (Huang et al., 2020; Li et al., 2018, Wei et al., 2018).

The aftereffects of corrosion damage on the mechanical properties of the steel reinforcement are significant and adequately reported by Apostolopoulos & Papadakis (2008). Corrosion in reinforced concrete

structures first manifests in the form of deterioration of steel bars in terms of loss of tensile and bond strengths, erosion of ribs, which weakens its ability to transfer the tensile stresses from concrete to steel. The progressive deterioration also extends to the surrounding concrete and manifests in the form of spalling of concrete cover because of the expansion of the corrosion products. The composite action of the steel and concrete is ultimately weakened by the loss of the interfacial bonding initiated by the lubricant effect of the corrosion products and by cracking of the concrete cover (Adewuyi et al. 2022; Maaddawy et al., 2005).

The strength and fracture behaviour of concrete are progressively affected by crack width and pattern, connectivity, and torsion. Timely and accurate diagnosis of these parameters helps to estimate the level of damage and reliably predict the residual service life of concrete (Brandt and Jozwiak-Niedzwiedzka, 2012). The stresses in the reinforcement at the cracked section at various load stages is a measure of the incidence of uniaxial tension and flexural cracking (Soltani et al., 2013). Hence, progressive cracking and loss of steel-concrete interfacial bonding in the form of slippage of steel rebars worsen the serviceability requirements of RC beams, and even much more by corrosion of reinforcement (Li et al., 2018; Siddika et al., 2020; Ballim et al., 2003).

Most short-term experimental studies on durability assessment of RC beams were based on accelerated corrosion. Since corrosion is a time-dependent phenomenon, accelerated laboratory corrosion tests are adopted to assess the effects of corrosion on the performance of RC structures in terms of the duration of exposure as well as the severity of the environmental conditions (Altoubat et al., 2016; Ballim et al., 2003; Fernandez et al., 2016; Malumbela et al., 2009; Słowik 2018, Zhang et al., 2018). Extensive studies have been conducted to monitor the effects of corrosion on various structural performance characteristics of RC flexural members such as mass loss, load-deflection pattern, stiffness and bond strength under ultimate load testing conditions. Ballim et al. (2003) reported 40–70% increase in deflections of tested beams relative to the deflection of the corresponding control samples when up to 6% of the mass of steel bars was lost to corrosion.

Maaddawy et al. (2005) found a 22% faster crack width propagation under sustained loading conditions than in an unloaded condition. It was reported that 8.9% and 22.2% rebars mass loss produced 6.4% and 20.0% strength loss, respectively. Fernandez et al. (2016) confirmed an increase in deflection and ductility in all corroded RC

beams under sustained service loading conditions during the corrosion phase. Yoon et al. (2000) recommended that the influence of service load on the structural performance of RC beams should be considered in combination with material properties and environmental conditions.

This study was primarily aimed at comparatively assessing the influence of M1 and M2 steel rebars on the flexural behaviour of RC beams, herein designated as B-M1 and B-M2, under normal and artificially induced corrosive environments. Better understanding of the relationship between the corrosion of rebars and integrity RC structures is essential to assist owners and managers of large-scale constructed concrete infrastructure to map out plans for maintenance and repairs strategies and efficient deployment of limited financial and human resources.

MATERIALS AND METHODS

The concrete used in this study consisted of PPC BOTCHEM cement of grade 32.5R of relative density 3.0. Coarse aggregate of 19 mm maximum nominal size and crusher dust as fine aggregate were sourced from Kgale Quarry Site. The water/cement ratio of 0.55 was adopted in the concrete mix. Twelve samples of simply supported RC beams each of dimensions 150 mm × 200 mm × 3000 mm of 30 N/mm² target concrete compressive cube strength at 28th day were cast, cured and tested for the experimental study. The beams were reinforced with M1 and M2 steel reinforcements and detailed as shown in Figure 2 and subjected to a sustained service loading to investigate the flexural behaviour under normal and artificially induced accelerated corrosion conditions.

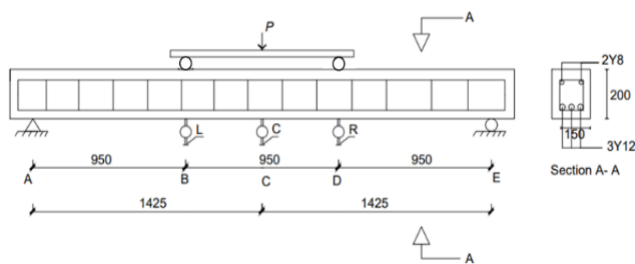


Figure 2. Four-point loading bending test setup for RC beams.

The beams were reinforced with three bars of 12 mm (3Y12) diameter high yield strength deformed (HYSD) steel bars at the tension zone, and 2 bars of 8 mm (2Y8) diameter hanger bars at the compression zone. The concrete nominal cover to longitudinal bars and shear links was 20 mm. Two-legged vertical shear stirrups of 8 mm nominal diameter size were provided at 125 mm

centres (Y8@125 mm). After casting and demoulding of concrete, all the test specimens were subjected to a 28 days of continuous curing condition at room temperature prior testing to ensure sufficient degree of hydration of the cement paste. The protruded rebar portions for the purpose of electrical connection for the accelerated corrosion procedure, were covered in 2 layers of insulating tape to prevent them from getting in contact with curing water and remain non-corroded.

Six RC beam specimens, three of which were separately reinforced with M1 and M2 steel rebars, were subjected to four-point bending test procedure under normal exposure condition. For the remaining six beams, three beam specimens were separately reinforced with M1 and M2 steel rebars. The three embedded tension rebars were separately subjected to an artificially induced accelerated corrosion process comprising a passage of constant current of 0.5 A through a DC power supply for the period of study. The lateral deflection under varying load intensity on the RC beams were measured by three dial gauges with accuracy to 0.01 mm and displacement transducers placed at the mid-span and at 950 mm from either supports and subjected to a sustained service load corresponding to 12 percent of the ultimate load for a 60-hour exposure duration and subsequently loaded progressively to failure. The beams were tested for four-point loading in a flexural testing frame. Line loads were applied equally at the third-points to either supports via the rollers from the load from the hydraulic jack centrally applied to a channel steel beam as shown in Figure 2 in accordance with ASTM C78 (2018). Crack microscope (of 0.02 mm resolution) was used to measure crack widths on the concrete surface under load increment. Crack length and width, on the other hand, were measured using crack metre as the applied load was progressively increased at a uniform load rate. The same procedure was employed under corrosive exposure condition.

A pond of size 150 × 700 × 50 mm placed at the top of the middle-third of the beam and containing 5% sodium chloride (NaCl) solution to accelerate corrosion process of the RC beams. A stainless-steel cathode was fixed on top of the beam over the length of 700 mm as shown in Figure 3. The brine, that is NaCl, solution was changed after every 3 hours to maintain the concentration of the aqueous solution. After sixty hours, dial gauges were set to zero, took off the pond and tested beam for flexural behaviour by loading beams at intervals of 0.25 tons using a hydraulic jack. Current-induced corrosion flowed from the positive terminals of the DC power supply to the tension reinforcements, and then through the saturated concrete

and sodium chloride solution to the stainless-steel plate which was connected to the negative terminals of the DC power supply. Tests were run by monitoring sustained load first for 60 hours to ensure that corrosion initiation takes place. Deflection and cracks of the RC beams were monitored under the sustained load.



Figure 3. Pond placed and sealed at the center of the beam for accelerated corrosion.

RESULTS AND DISCUSSION

Flexural behaviour of RC beams with M1 and M2 rebars in a non-corrosive environment

The load-deflection plots in Figure 4(a) shows higher deflection at midspan, where B-M1 recorded a maximum deflection of 39.8 mm at midspan and 35.4 mm at one third point at an ultimate failure load of 63.8 kN. Beam B-M2 had a higher load carrying capacity of 68.7 kN with a corresponding deflection of 34.5 mm at midspan and 34.1 mm at one third point. The higher failure load recorded in B-M2 than B-M1 could be attributed to the higher yield strength of 459 N/mm² for M2 compared to the 427 N/mm² recorded for M1. During the progressive loading-initiated cracking, B-M1 had its first cracking load at 17.2 kN, while B-M2 experienced early cracking at 9.8 kN. This was almost twice the first cracking load of B-M1. Loss of flexural rigidity of the all the beam specimens was obvious after the occurrence of the first crack, and each specimen began to exhibit a lower second order stiffness and entirely different structural behaviours. The stiffness of B-M1 at midspan changed from 1.9 to 1.4 which was a slight change as compared to stiffness of B-M2 which significantly changed from 4.9 to 3.1.

A similar trend at one third span was followed for both B-M1 and B-M2 as shown in Figure 4(b). The stiffness for B-M2 reduced by 67% after first crack hence bringing the total deflection to 34 mm which is closer to 35 mm of B-M 1. Low load rate was employed in the study because it has been established by Li et al. (2018) that a higher loading level decreases flexural stiffness of RC beams, while a lower loading rate produces a relatively higher flexural stiffness. The ductility ratio of a flexural test is often determined as the ratio of the ultimate curvature to the yield curvature of a section. In this study, however, the ductility ratios were measured as a function of the ratio of deflection at ultimate load to the corresponding value at the instance of first cracks. The ratio of the first crack to ultimate failure were 26.9% and 14.3% for B-M1 and B-M2 respectively. The ratio implies that B-M2 was more ductile since B-M1 could only resist load to about 73% and B-M2 about 86% after the first crack observation. Ridha et al. (2018) attributed the relatively lower values of ductility ratio recorded in the experimental programme to the brittleness of the tested RC beams.

The mode of ultimate failure of B-M1 was flexural tension failure with crushed concrete in the compression zone. However, beams B-M2 had diagonal shear tension failure as shown in Figure 5. For the flexural failure scenario, there was a progressive deflection which began as a set of parallel tiny vertical cracks that progressed as the beam was subjected to a gradually increasing load and terminated as crushing of the concrete within the vicinity of the point of maximum moment (Li et al., 2018). However, in the case of shear mode of failure, the first crack appeared vertically on the side surface at the midspan of beams. As the load increased at a slow, but constant rate, inclined or diagonal cracks were initiated at the shear-flexural zone near the support point, which incidentally the point of maximum shear, and gradually progressed toward the third point of load application.

The ultimate failure occurred quite suddenly as the inclined cracks widened up from left end of the support and propagated towards the point of load application by the roller at the third point of the beam. The results of shear failure could be related to point load being shifted to the left since the load was applied manually by the jack. The shear span to depth ratio was higher which supports that the reinforcement used was sufficient to resist shear (Abigaz, Liu & Yilachew, 2021). The shear failure could be related to reinforcement that was used for shear, had low rib height and no gaps which could temper with bond between concrete and reinforcement.

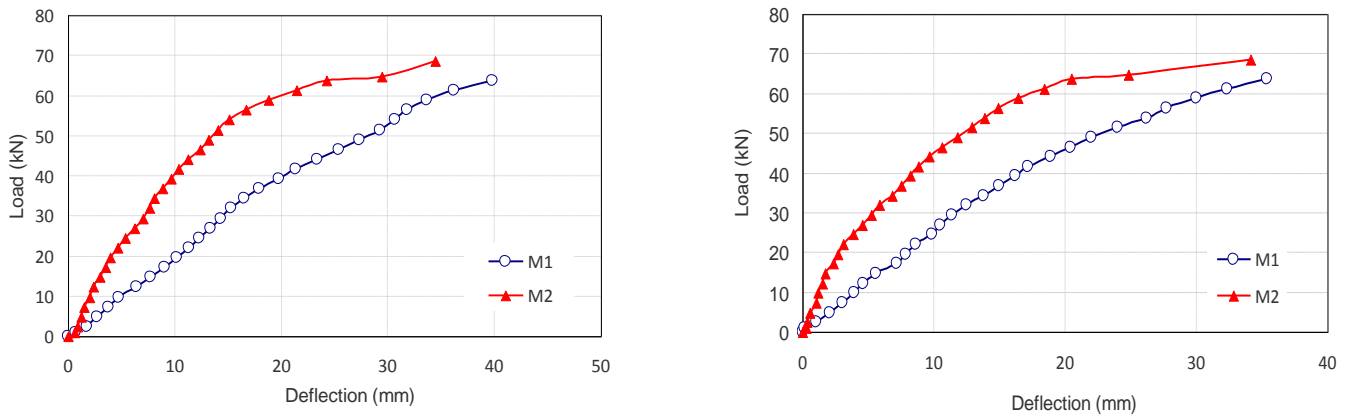


Figure 4. Load- deflection curves of RC beams embedded with M1 and M2 steel bars at (a) midspan and (b) one-third span.



Figure5. Flexural test failure patterns of controlled specimens of RC beam reinforced with (a) M1 and (b) M2 at ultimate failure

Flexural behaviour of corrosion-induced RC beams with M1 and M2 steel bars

Deflection and cracks were monitored consistently at an interval of 3 hours for 60 hours. No cracks were recorded for all beams under sustained loading. This could be because the sustained load was lower than the initial first cracking load when non corroded beams were tested. Steel reinforcing bars embedded could have not

corroded enough to cause any crack as the corrosion products are expected to expand and cause cracking of concrete beams. Deflection values were slightly low as shown in Figure6. The deformation of the RC beams under sustained loading is linearly elastic as revealed by the almost linear deflection- time graphs.

The midspan deflection under sustained loading for M1 ranged between 0.715 mm to 0.978 mm at a rate of

0.0034 mm/hr, while the corresponding deflection for M2 ranged from 0.878 mm and 1.104 mm with a slope of 0.0041 mm/hr for the entire 60 hours duration. On the other hand, the deflection measurements at one-third points of beams M1 and M2 are practically comparable ranging between 0.369 mm and 0.576 mm at a rate of 0.0037 mm/hr for the 60 hours monitoring duration. This shows that the corroding RC beams were still under elastic deformation hence slight changes in the first crack formation when the beams were then tested under third point loading until failure. In overall, the flexural failure modes of the specimens which is common and highly recommended, was characterized by the yielding of steel rebars, multiple micro cracks, and lastly crushing which agrees to results obtained by Qiu et al. (2022).

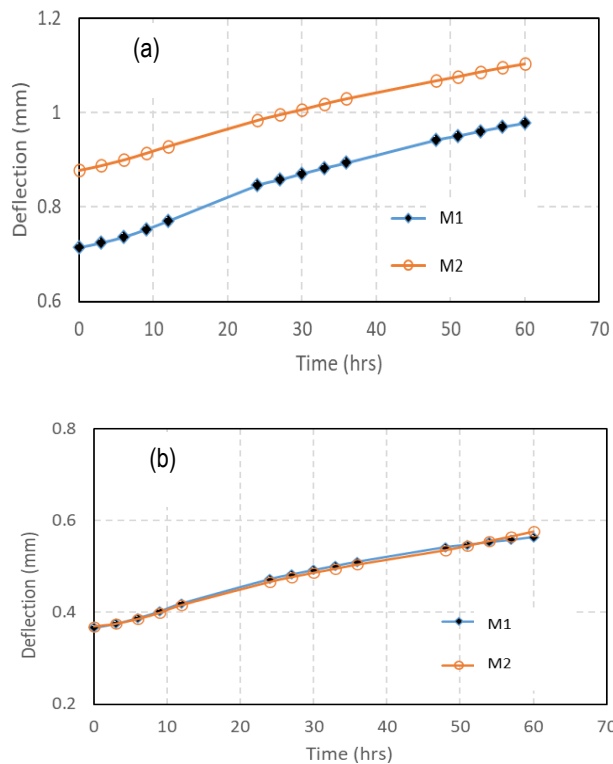


Figure 6. Deflection of the RC beams under sustained loading at (a) the midspan and (b) one third span.

After 60 hours of sustained loading, RC beams were unloaded from the sustained loading then set dial gauges to zero so as to load beams from zero until failure load. The load-deflection plots for RC beams subjected to corrosion in Figure 7 show relatively high deflection at midspan, where B-M1 had a failure load of 54.0 kN with a corresponding deflection of 47.3 mm at midspan and 41.1 mm at quarter span whereas B-M2 had the highest failure

load of 64.7 kN with a corresponding deflection of 41.8 mm at midspan and 38.5 mm at one third point. Steady load-initiated cracking in which B- M1 had its first crack noticed at 12.3 kN, while B-M2 experienced its first cracking at 14.7 kN. The rigidity of the beam test specimen decreased immediately after the first crack initiated. Afterwards, each RC beam test specimens began to have a different behaviour with a much lower flexural stiffness.

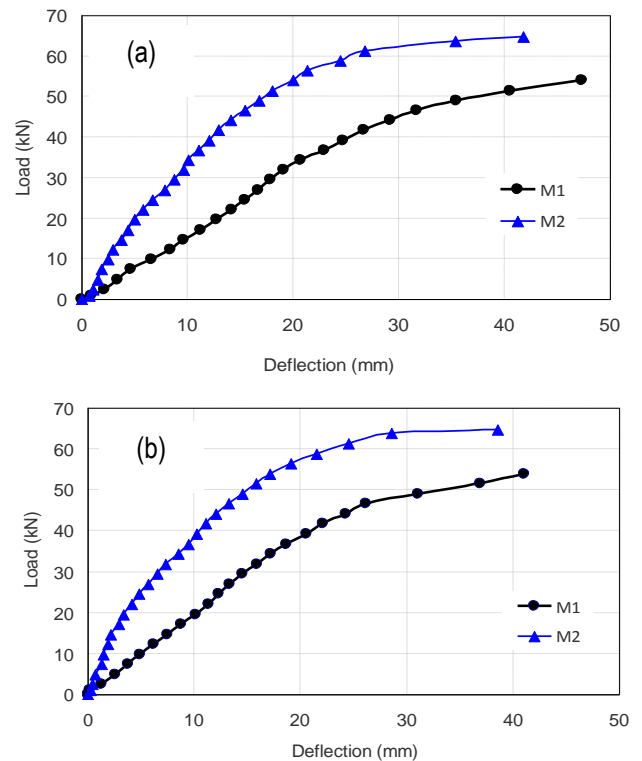


Figure 7. Load-deflection curves of corrosion induced RC beams at (a) midspan and (b) one-third span.

The stiffness before first crack of B-M1 at midspan was twice smaller than stiffness of B-M2 hence low deflection for B-M1 than B-M2. The stiffness after first crack followed the same trend at midspan. However, at one third span, the stiffness for B-M1 was constant before and after first crack. The stiffness for B-M2 reduced by 50% after first crack hence reducing deflection at one third span. The percentage of the first crack load to the ultimate failure were both relatively low. B-M1 had 26.9% residual capacity after the first crack, while rattan RC beams had exhausted 14.3% of its load-carrying capacity after the first crack.

With an increase in cracking and possible bond slippage there is increase the serviceability deflections of a reinforced concrete (RC) beam which has deteriorated

because of corrosion of reinforcement (Ballim et al., 2003). The failure mode of both B-M1 and B-M2 flexural tension failure with more cracks noticed at midspan and few at the outer span as shown in Figure 7. The most significant failure modes in this study are the shear and flexural failures. However, flexural failure mode is preferred to shear failure due to brittleness and catastrophic failure form of the shear failure, because it allows the possibility of stress redistribution. Full advantage of the potential ductility of the RC members can be achieved by selecting geometric properties of concrete sections and tensile strength of steel reinforcing bars that would guarantee flexural failure mode instead of the sudden, brittle and catastrophic shear failure, which occurs with no advance warning of distress.

Comparison of flexural behaviour RC beams embedded with M1 and M2 rebars at midspan under normal and corrosive induced environmental conditions

The results of beams before introducing corrosive environment (M1-norm and M2-norm) and during induced corrosion (M1-corr and M2-corr) were compared in Figure 8. The results showed an increase in deflection and decrease in ultimate load after beams have been exposed to corrosion. It was evident from the study that corrosion of the longitudinal steel rebars manifested in the form of mass loss and strength loss which reduced the slope and the geometric properties of the load-deformation curve of RC beams. These translated into a general reduction in ductility, flexural stiffness, and bending strength. The bending strength of B-M1 reduced from 48.49 N/mm² to 41.04 N/mm² while B-M2 reduced from 52.21 N/mm² to 49.17 N/mm².

This shows that B-M2 could resist failure in bending better than B-M1 even after beams were exposed to corrosion. This shows reduction in strength for B-M1 and B-M2 to be 15.4% and 5.8% respectively in terms of percentage of corroded failure load to normal failure load. After subjecting RC beams to accelerated corrosive condition, the percentage ratio of the first crack load to the ultimate failure load for B-M1 decreased from 86% to 65%, while B-M2 increased from 73% to 81.7%. Comparing the failure load values and deflection values, it is evident that the non-corroded steel-RC beam performed better in resisting bending than the corroded steel-RC beam, and thus demonstrating that corrosion adversely affects the flexural strength of reinforced concrete. In conclusion, a significant reduction in the load-carrying capacity and an inversely proportional increase in

corresponding deflection. This invariably severely reduced the RC structural performance at various service load levels. The most technical factor that can be attributed to this deterioration trend was simply the loss of stiffness due to reduction in steel geometric cross-section as well as yield and ultimate tensile strength. It is quite clear that deflections are strongly influenced by corrosion of steel (Fernandez et al., 2016). This is because there is an increase in deflection as RC beams get exposed to corrosive environment for all the RC beams.

CONCLUSION

The flexural behaviour of RC beams reinforced with B-M1 had a lower flexural strength for both normal beams and beams under corrosive environment as compared to B-M2. The flexural strength of B-M1 had reduced from 48.49 N/mm² to 41.04 N/mm² while B-M2 reduced from 52.21 N/mm² to 49.17 N/mm². This was proven by higher failure loads of B-M2. In addition, this links to high tensile strengths obtained in steel bar specimen of M2. The results showed a decrease in stiffness after first crack for all samples. The mode of failure experienced by 75% of the beams was flexural tension failure at ultimate failure load. The signs of this type of failure were development of cracks at the tension side of the beam which further extend to the compression side. These cracks are mostly vertical and located at the middle third of the beam. Great deflection is another sign of flexural tension failure as it was expected. One-quarter of the tested beams failed by diagonal tension shear without any warning of impending failure. The research revealed that corrosion reduces the flexural strength and increases the ductility of RC beams. M2-RC beams exhibited higher strength compared to M1-RC beams under the normal and corrosive exposure conditions. The loss of flexural capacity to similar exposure to corrosion for B-M1 and B-M2 were 15.4% and 5.8% respectively. This is partly connected to the slightly higher tensile strength and relative rib areas of M2 reinforcing bars.

DECLARATIONS

Corresponding Author

Correspondence and requests for materials should be addressed to Adekunle P. Adewuyi; Email: AdewuyiA@ub.ac.bw; ORCID: 0000-0001-8190-7357

Data availability

The datasets used and/or analysed during the current study available from the corresponding author on reasonable request.

Acknowledgements

The authors would like to acknowledge the Office of Research and Development of the University of Botswana for the internal funding for this research project R1207. The technical staff of the Structural Engineering Laboratory of the Department of Civil Engineering are also appreciated for their support and for creating a conducive environment to conduct this research.

Authors' contribution

AP Adewuyi originated the research concept, identified the research gaps in the existing literature, designed the experimental process, analysed the data, and revised the manuscript. **GB Eric** developed the proposal, conducted the laboratory experimental study, analysed the results and wrote the manuscript. Both authors read and approved the final manuscript

Competing interests

The authors declare no competing interests in this research and publication.

REFERENCES

- Adewuyi, A.P., Eric, G.B., and Kanyeto, O.J. (2022) Characterization of major reinforcing bars for concrete works in Botswana construction industry, *Current Perspectives and New Directions in Mechanics, Modelling and Design*. <https://doi.org/10.1201/9781003348443-203>
- Adewuyi, A.P., Otukoya, A.A., Olaniyi, O.A. and Olafusi, O.S. (2015). Comparative studies of steel, bamboo and rattan as reinforcing bars in concrete: tensile and flexural characteristics. *Open Journal of Civil Engineering*, 5(2), 228-238. <https://doi.org/10.4236/ojce.2015.52023>
- Almusallam, A. (2001). Effect of degree of corrosion on the properties of reinforcing steel bars. *Construction and Building Materials*, 15(8), 361-368. [https://doi.org/10.1016/S0950-0618\(01\)00009-5](https://doi.org/10.1016/S0950-0618(01)00009-5)
- Altoubat, S., Maalej, M. and Shaikh, F.U. (2016). Laboratory simulation of corrosion damage in reinforced concrete. *International Journal of Concrete Structures and Materials*, 10(3), 1-9. <https://doi.org/10.1007/s40069-016-0138-7>
- Apostolopoulos, C.A. and Papadakis, V.G. (2008). Consequences of steel corrosion on the ductility properties of reinforcement bar. *Construction and Building Materials*, 22(12), 2316-2324. <https://doi.org/10.1016/j.conbuildmat.2007.10.006>
- ASTM C78 - 09 (2010). Standard test method for flexural strength of concrete (Using simple beam with third-point loading). ASTM International, West Conshohocken.
- Ballim, Y., Reid, J.C. and Kemp, A.R. (2003). Deflection of RC beams under simultaneous load and steel corrosion. *Magazine of Concrete Research*, 55(4), 405-406. <https://doi.org/10.1680/mac.2003.55.4.405>
- Brandt, A.M. and Jóźwiak-Niedźwiedzka, D. (2012). Diagnosis of Concrete Quality by Structural Analysis. ASTM International. *Advances in Civil Engineering Materials*, 1(1): ACEM20120004. <https://doi.org/10.1520/ACEM20120004>
- Bertolini, L., Elsener, B., Pedferri, P. and Polder, R. (2013). *Corrosion of Steel in Concrete: Prevention, Diagnosis, and Repair*, 2nd Edition. Weinheim: Wiley-VCH. <https://doi.org/10.1002/9783527651696>
- Djamaluddin, R. (2013). Flexural behaviour of external reinforced concrete beams. *Procedia Engineering*, 54, 252 - 260. <https://doi.org/10.1016/j.proeng.2013.03.023>
- Fernandez, I., Herrador, M.F., Marí, A.R. and Bairán, J.M. (2016). Structural effects of steel reinforcement corrosion on statically indeterminate reinforced concrete members. *Materials and structures*, 49, 4959 - 4973. <https://doi.org/10.1617/s11527-016-0836-2>
- Fouad, N., Saifelddeen, M. A., Huang, H. & Wu, Z. S. (2016). Early corrosion monitoring of reinforcing steel bars by using long-gauge carbon fiber sensors. *Journal of Civil Structural Health Monitoring*, 6, 691-701. <https://doi.org/10.1007/s13349-016-0190-7>
- Huang, L., Ye, H., Jin, X., Jin, N. & Xu, Z. (2020). Corrosion-induced shear performance degradation of reinforced concrete beams. *Construction and Building Materials*, Elsevier, 248(1), p. 118668. <https://doi.org/10.1016/j.conbuildmat.2020.118668>
- Hunkeler, F. (2005). Corrosion in reinforced concrete: Processes and mechanisms. Cambridge: Woodhead Publishing Limited. <https://doi.org/10.1201/9781439823439.ch1>
- Ignjatovic, I. S., Marinkovic, S. B., Miskovic, Z. M. & Savic, A. R. (2013). Flexural behavior of reinforced recycled aggregate concrete beams under short-term loading. *Materials and Structures*, 46, 1045-1059. <https://doi.org/10.1617/s11527-012-9952-9>
- Kim, S. & Kim, S. (2019). Flexural Behavior of concrete beams with steel bar and FRP reinforcement. *Journal of Asian Architecture and Building Engineering*, 18(2), 89-97. <https://doi.org/10.1080/13467581.2019.1596814>
- Kunawisarut, A., Iwanami, M., Chijiwa, N. and Nakayama, K. (2024). Assessment of bond deterioration in corroded RC members incorporating cracking response and tension stiffening. *Structure and Infrastructure Engineering*, 20(4): 581-593. <https://doi.org/10.1080/15732479.2022.2131843>
- Li, H., Li, B., Jin, R., Li, S. and Yu, J. G. (2018). Effects of sustained loading and corrosion on the performance of reinforced concrete beams. *Construction and Building Materials*, 169, 179-187. <https://doi.org/10.1016/j.conbuildmat.2018.02.199>
- Li, Q., Guo, W., Liu, C., Kuang, Y. and Geng, H. (2020). Experimental and theoretical studies on flexural performance of stainless steel reinforced concrete beams. *Advances in Civil Engineering*, 2020(1), 4048750. <https://doi.org/10.1155/2020/4048750>
- Maaddawy, T. E., Soudki, K. and Topper, T. (2005). Analytical Model to Predict Nonlinear Flexural Behavior of Corroded RC beams. *ACI Structural Journal*, 102(4): 550-559. <https://doi.org/10.14359/14559>

- Makul, N. (2020). Advanced smart concrete - A review of current progress, benefits and challenges. *Journal of Cleaner Production*, 274(20): 122899. <https://doi.org/10.1016/j.jclepro.2020.122899>
- Malumbela, G., Moyo, P. and Alexander, M. (2009). Behaviour of RC beams corroded under sustained service loads. *Construction and Building Materials*, 23(11). 3346-3351. <https://doi.org/10.1016/j.conbuildmat.2009.06.005>
- Patil, A. N., Birajdar, B. G. and Dawari, B. M. (2017). Influence of corrosion on flexural strength of concrete. *Journal of Structural Engineering and Management*, 4, 35-42.
- Peng, L., Zhao, Y. and Zhang, H. (2021). Flexural behavior and durability properties of recycled aggregate concrete (RAC) beams subjected to long-term loading and chloride attacks. *Construction and Building Materials*, 277(29). 122277. <https://doi.org/10.1016/j.conbuildmat.2021.122277>
- Qiu, M., Hu, Y., Shao, X., Zhu, Y., Li, P. and Li, X. (2022). Experimental investigation on flexural and ductile behaviors of rebar-reinforced ultra-high-performance concrete beams. *Structural Concrete*, 23(3). 1533-1554. <https://doi.org/10.1002/suco.202100794>
- Ridha, M., Sarsam, K. and Al-Shaarbaf I. (2018). Experimental study on shear resistance of reactive powder concrete beams without stirrups. *Mechanics of Advanced Materials and Structures*, 27(12). 1006-1018. <https://doi.org/10.1080/15376494.2018.1504258>
- Rodrigues, R., Gaboreau, S., Gance, J., Ignatiadis, I. and Betelu, S. (2021). Reinforced concrete structures: A review of corrosion mechanisms and advances in electrical methods for corrosion monitoring. *Construction and Building Materials*, 269(1). 121240. <https://doi.org/10.1016/j.conbuildmat.2020.121240>
- Siddika, A., Al Mamun, A., Ferdous, W. and Alyousef, R., (2020). Performances, challenges and opportunities in strengthening reinforced concrete structures by using FRPs - A state-of-the-art review. *Engineering Failure Analysis*, 110(1): 104480. <https://doi.org/10.1016/j.engfailanal.2020.104480>
- Soltani, A., Harries, K.A. and Shahrooz, B. (2013). Crack opening behavior of concrete reinforced with high strength reinforcing steel. *International Journal of Concrete Structures and Materials*, 7(4): 253-264. <https://doi.org/10.1007/s40069-013-0054-z>
- Słowik, M. (2018). The analysis of failure in concrete and reinforced concrete beams with different reinforcement ratio. International Centre for Settlement of Investment Disputes 89, 885-895. Washington: *Archive of Applied Mechanics*. <https://doi.org/10.1007/s00419-018-1476-5>
- Verstrynghe, E., Van Steen, C., Vandecruys, E. and Wevers, M. (2022). Steel corrosion damage monitoring in reinforced concrete structures with the acoustic emission technique: A review. Steel corrosion damage monitoring in reinforced concrete structures with the acoustic emission technique: A review, 349(26). p. 128732. <https://doi.org/10.1016/j.conbuildmat.2022.128732>
- Wei, Y., Wu, Z., Huang, J. and Liang, S. (2018). Comparison of compressive, tensile, and flexural creep of early-age concretes under sealed and drying conditions. *Journal of Materials in Civil Engineering*, 30(11). p. 04018289. [https://doi.org/10.1061/\(ASCE\)MT.1943-5533.0002495](https://doi.org/10.1061/(ASCE)MT.1943-5533.0002495)
- Yoon, S., Wang, K., Weiss, J.W. and Shah, S.P. (2000). Interaction between loading, corrosion, and serviceability of reinforced concrete. *ACI Structural Journal*, 97(6), 637-644. <https://doi.org/10.14359/9977>
- Zhang, W., Zhang, H., Gu, X. and Liu, W. (2018). Structural behavior of corroded reinforced concrete beams under sustained loading. *Construction and Building Materials*, 174, 675-683. <https://doi.org/10.1016/j.conbuildmat.2018.04.145>

Publisher's note: [Scienceline Publication](#) Ltd. remains neutral with regard to jurisdictional claims in published maps and institutional affiliations.



Open Access: This article is licensed under a Creative Commons Attribution 4.0 International License, which permits use, sharing, adaptation, distribution and reproduction in any medium or format, as long as you give appropriate credit to the original author(s) and the source, provide a link to the Creative Commons licence, and indicate if changes were made. The images or other third party material in this article are included in the article's Creative Commons licence, unless indicated otherwise in a credit line to the material. If material is not included in the article's Creative Commons licence and your intended use is not permitted by statutory regulation or exceeds the permitted use, you will need to obtain permission directly from the copyright holder. To view a copy of this licence, visit <https://creativecommons.org/licenses/by/4.0/>.